J Mater Sci (2007) 42:1828–1832
DOI 10.1007/s10853-006-0695-2

Characterization of soft magnetic nano-material deposited with M^{3}D technology

Michael Carter · Tony Amundson · Jacob Colvin · James Sears

Received: 18 April 2006 / Accepted: 20 July 2006 / Published online: 30 January 2007

Abstract Direct Write Technologies are being utilized in antennas, engineered structures, sensors, and tissue engineering. One form of Direct Write Technology is Maskless Mesoscale Material Deposition (M^{3}D). The M^{3}D process is a process that uses aerosol formation, transport and deposition. Inks for the M^{3}D process utilize nano-particles in suspension for deposition. Soft magnetic material was formulated as an ink suspension, deposited and characterized.

This paper will report on the results obtained after depositing the soft magnetic material. The results of the permeability are calculated from magnetic structures created with the deposition. These results are compared to conventional methods of soft magnetic material formation and construction.

M^{3}D Technology

The DARPA MICE program introduced four new technologies to make micron sized electrical circuits without the lithographic process. To meet the requirements of the project techniques must have the ability to deposit many types of materials on many different substrate materials and shapes. The four technologies developed because of the MICE program are: Direct write syringe process (MicroPen, n-Scrypt), Thermal spraying, Matrix Assisted Pulsed Laser Evaporation (MAPLE), and Maskless Mesoscale Material Deposition (M^{3}D). These four technologies have been developed in the past decade and are being introduced for market penetration.

Optomec and their MICE partners created the M^{3}D technology and it became commercially available in 2004. The M^{3}D system is designed for rapid prototyping of electronic equipment, legacy repair, and other novel experimental uses. The M^{3}D process utilizes a basic three-step procedure in its depositions: aerosolization, deposition, and heat-treatment of the deposition.

With the M^{3}D process, feature definitions of 10 microns are realized [1]. The M^{3}D system is maskless, eliminating the need for expensive and fragile masks. The M^{3}D system is able to do conformal coating and three-dimensional builds. Any substance can be deposited if it can be made into a liquid with a viscosity less than 1000 cp [2]. M^{3}D can deposit a wide assortment of materials, including biological, on a wide array of substrates [3]. The laser processing can be done in situ, reducing the amount of infrastructure required. The M^{3}D process can deposit at speeds of 200 mm per second [3]. A laser guided deposition system using the same principles, using a laser instead of an air stream to guide the materials, was also created. The laser-guided system has higher feature resolution than the air stream guided, but is not used in industrial settings [4]. Both deposition methods have

M. Carter
Department of Material and Metallurgical Engineering, South Dakota School of Mines and Technology, Rapid City, SD 57701, USA

T. Amundson
Department of Electrical and Computer Engineering, South Dakota School of Mines and Technology, Rapid City, SD 57701, USA

J. Colvin (✉) · J. Sears
Additive Manufacturing Laboratory, South Dakota School of Mines and Technology, Rapid City, SD 57701, USA
e-mail: jacob.colvin@sdsmt.edu

been used to deposit biological cells [5, 6]. The largest benefit of the M^3D system is the ability to directly read CAD files, allowing simple transfer from design to deposition [7].

The M^3D process does have limitations. The volumetric deposition rate is not as high as the other MICE technologies. The workspace in the system is currently 300 mm by 300 mm, limiting the overall size of the substrate [2]. All deposition materials must be in a liquid form with a viscosity under 1000 cp, which requires rheological knowledge of the slurry/ink to be deposited. Viscosity can be modified by increased dilution rates.

Initially, the viscosity of the material to be deposited is determined in preparation for aerosolization. Materials with a viscosity of less than 10 cP are atomized with an ultrasonic atomizer, utilizing an ultrasonic puck to create the aerosol. Materials with a higher viscosity are atomized with a pneumatic atomizer, which can atomize fluids with a viscosity up to 1000 cP. Solvents can be used to adjust the viscosities of liquids. Many off the shelf materials can be used for the M^3D process as well as many novel materials.

In the second process step, deposition, the aerosol created in the first step is entrained in an air stream and carried to the deposition head. If the aerosol was created with the pneumatic atomizer, it must pass through a virtual impactor to size sort the aerosol droplets. Due to the narrow variance of size distribution of ultrasonically created aerosols, they do not have to pass through the impactor. The entrained aerosol then passes to the deposition head, through a heating element to heat the air stream to temperatures up to 150 °C. After the air leaves the heating tube, it goes to the collector, which focuses the air flow to a tight point for deposition. The focused air travels through a final nozzle, and is then deposited upon a substrate. For optimal conditions the nozzle should stand off from the substrate 1–5 mm. The material is impacted subsonically to the substrate. To assist with the adhesion of the deposition to the substrate, the substrates can be treated with hydrophilic or hydrophobic solutions for various solvents and materials.

The third step, thermal treatment of the depositions (sintering), is used to achieve actualization of the component designs by promoting solid state diffusion in the deposited materials. Thermal treatment, either in an oven or through laser processing, is necessary to remove excess solvent, and to remove material impurities from the depositions. Both oven and laser thermal treatments accomplish sintering of the depositions, producing resistivity close to that of bulk metals [6]. The thermal treatment provides a secondary benefit of improving the bond of the deposition to the substrate. A heating element embedded in the substrate platen is used in the M^3D system to elevate the temperature of the substrate during the deposition allowing for in situ heat treatment.

Construction of a soft magnetic based inductor

The M^3D system has been used to deposit conductive silver inks developed at the South Dakota School of Mines and Technology [8–10]. Magnetic materials are required for many electronic devices, and there is currently no commercially available soft magnetic material designed for the M^3D process. A novel soft magnetic material, a permalloy analog, was created, and formulated for deposition with the M^3D system. A rudimentary nine and a half turn inductor was created, utilizing a silver ink known as V2 as the conductor. There are other cases of direct written inductors fabricated with the M^3D process in the literature. These include yttrium iron garnet core inductors [11] and manganese zinc ferrite cored inductors [12]. What makes this inductor unique is the fact that it utilizes a soft magnetic nickel based material, which is a cost improvement over the previous inductor materials. The primary constituents of the core are nickel and iron oxide, both of which are relatively common and inexpensive materials. The key step in the creation of the inductor is the removal of the oxygen from the iron and the alloying of the nickel and the oxygen free iron. This alloying is done at a low temperature, ~50% of that of the bulk materials, allowing for lower temperature substrates and lower energy of formation requirements.

Several trial inductors were made to verify the optimum parameters for such a deposition. Initial problems included alignment issues and alloying of magnetic material with the conductive deposited silver. The alignment issues were rectified with the utilization of an onboard alignment system on the M^3D machine. This allowed the creation of deposits with a tolerance of less than 5 microns, greatly increasing the efficiency of the manufacturing. To prevent the alloying of the silver with nickel particles in the magnetic ink, a barrier dielectric material was needed. The silver–nickel alloy has a much lower conductivity than pure silver, and the higher resistivity disrupts the function of the inductor. The initial barrier used was a combination of Matrimid 5292 A and Matrimid 5292 B, purchased from Huntsman Advanced Materials and modified for use with the M^3D system. The dielectric material did provide an effective barrier layer between the silver and nickel components. A dielectric material constructed from muscovite mica was also used in the fabrication of the inductors and was found to be easier to work with and to give superior results to the Matrimid process.

The inductors were constructed in a five step process. The first step involved the creation of contact pads and lines for the bottom of the inductor core. The second step was to place a barrier dielectric layer over the area where the core material would be placed. The third step was the deposition of the core material. The core material deposition is the most time intensive step. A layer of dielectric was applied over the magnetic core for the fourth step, and the fifth step involved the completion of the silver lines that formed the turned wires for the inductor. The maximum temperature reached during the construction of the inductor was 500 °C. Figure 1 shows the deposition processes at various steps.

The ability to functionalize the inductor at 500 °C allows for low temperature sintering. The melting point of the permalloy is 1440 °C. A standard rule of thumb for a fully sintered powder construct is 80% of the melting temperature. This allows means that due to the method of fabrication of the permalloy, it sinters at 54% of the expected temperature. The 500 °C sintering was done with glass substrates, and an inductor was also deposited on 5 mil Kapton and sintered at 350 °C. This is 43% of the expected sintering temperature, a vast improvement allowing the use of lower temperature materials.

The physical dimensions of the inductor are 8 mm wide by 20 mm long. The thickness of the inductor was measured with a Keyence LT 9001 laser profilometer. The thickness of the magnetic material layers combined with the dielectric layers was an average of 29.75 microns thick. The maximum thickness of the inductors doesn't exceed 70 microns, leaving it with a much lower profile than other direct written inductors [11, 12]. The profilometer data from a scan of the inductor lengthwise is shown in Fig. 2. The high spikes

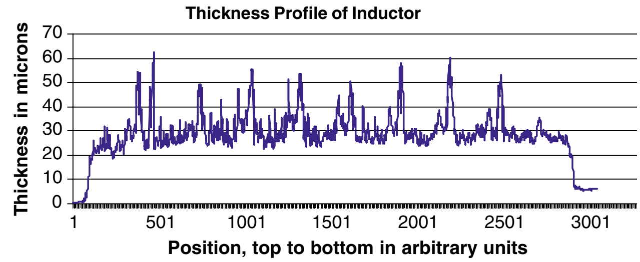

Fig. 2 Thickness profile of completed inductor. *X*-axis is arbitrary units of marking for profilometer position

are due to the silver lines, both under and over the magnetic material.

Testing of the inductor and magnetic properties

The testing of the magnetic properties and the inductance of the inductors were done with indirect methods. The use of indirect methods was required due to the equipment available. The inductor was placed in series with a resistor in a circuit, and the circuit was provided with stimuli. The results were logged, statistically analyzed and compared to theoretical models generated by Pspice, a common circuit simulator program. The equipment used in the experiments included a Tektronix CFG250 waveform generator, a Tektronix TDS2012 oscilloscope, and a FLUKE 87 digital multi-meter.

The circuit was assembled, and the voltages at the two resistor terminals (V_1 and V_2) were measured for varying frequencies. At each frequency the peak to peak time between V_1 and V_2 (Δt) was also measured. Due to the high ratio of the internal resistance of the function generator to the equivalent resistance of the circuit, the voltage V_1 varies slightly even though V_1 is connected directly to the source. This is acceptable for this method of measurement though, and will have no bearing on the final analysis, as this method uses the ratio of V_1 to V_2. To further reduce error, two sets of trials were performed, one at a higher voltage and current (1.2 V)

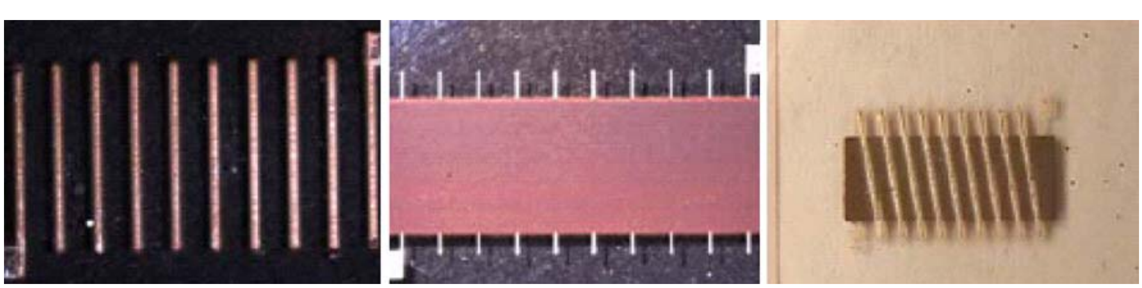

Fig. 1 Various stages of the inductor as it is being constructed

Table 1 Static characteristics of the R_L circuit

Characteristic	Value (Ω)
R_R	61.9
R_L	19.1
R_I	20,100

R_R, resistance of the resistor; R_L, resistance of the inductor and R_I resistance internal to the function generator

and one at a lower voltage and current (0.4 V) value for V_1. The frequencies for the lower voltage data set were limited to higher frequencies, where the inductor's impedance affected the measurement.

To experimentally determine the inductance (L) of the inductor, the circuit was analyzed as follows. A model was set up that contained an AC source of magnitude V_1 and with 0 degrees of phase shift. The source was connected in series through resistors of value R_R and R_L given in Table 1, in that order, and then through the inductor. This model replaces the actual inductor with an ideal inductor of equal inductance, and a resistor of value R_L. V_2 is located between the two resistors. AC circuit analysis was performed using Eqs. 1 and 2.

$$\frac{V_2\angle\phi}{V_1\angle 0^\circ} = \frac{(Lj\omega 2\pi + R_L)}{(Lj\omega 2\pi + R_L + R_R)} \quad (1)$$

$$\phi = 360\Delta t\omega \quad (2)$$

where V_1 is the magnitude of voltage at node 1 (volts); V_2 the magnitude of voltage at node 2 (volts); ϕ the phase shift (degrees); L the inductance (henries); $j = \sqrt{1}$ (dimensionless); ω the frequency (Hz); Δt the peak to peak time delay between V_1 and V_2 (s).

Ideally, when Eqs. 1 and 2 are applied, the non real numbers and phasors in the equations would left L with only a real component. Any slight deviation in the measurement of Δt, V_1, or V_2 will cause the imaginary component of L to be nonzero. The largest source of error in this experiment is in the measurement of Δt. This is due to the ratio of Δt to the inverse of the frequency, ω, approaches zero for low frequencies, and quickly falls below the resolution of the oscilloscope used. To correct for this error, statistical filtering methods were applied.

Statistical analysis and comparison to modeling

Statistical analysis was used to account for the error in measurement of the phase shift induced by the inaccurate transition period between 10 and 100 kHz. Since the precision of phase shift measurements was inversely proportional to the period, and thus directly proportional to the frequency, a method was used that takes into account the period. A common method that uses this principle of dealing with the period is simply setting to zero all measurements where the phase shift (in seconds) is less than a certain percentage of the total period (also in seconds.) The cutoff chosen was 1%, so all phase shifts of less than 3.6 degrees were truncated to zero for a combination of reasons including: they are close enough to zero that the impedance is minimal; they are values of low precision, with variances of up to +/–50%. The values for less than 10 kHz had the same criteria applied, and the phase shift was too small to be detected on the oscilloscope used. Figure 3 shows both the filtered and unfiltered results on a plot of inductance versus frequency.

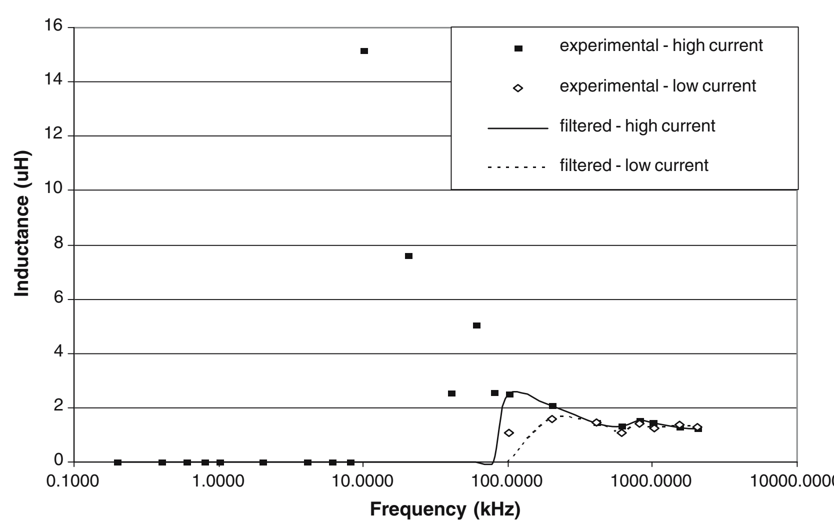

Fig. 3 Chart showing inductance versus frequency, with and without statistical filtering

From Fig. 3 the assumptions made concerning values below 100 kHz were justified. At values larger than 100 kHz, the inductance appears to be constant at approximately 1.5 uH. The analysis at both voltage values converges to the same value. An average of all remaining inductance values after the statistical filtering yields an inductance value of 1.478 uH.

A computer model utilizing the same circuit analysis technique as the experimental method was constructed. The model was constructed on PSpice version 9.1 utilizing an inductor of 1.478 uH. To show the similarity between the two circuits, the computer generated outputs for V_1 and V_2 were plotted at various frequencies. The predicted values were then compared with the experimental results. The close agreement (less than 5% deviation) of the model with the experimental results validates the experimental results and methods.

From the inductance of the inductor, along with the size and shape of the magnetic layer of the inductor allows for the back calculation of the relative magnetic permeability. From the inductor that produced theses results, a relative magnetic permeability of 625 was calculated. This relative magnetic permeability will help aid in the design of future components that utilize this material. Other inductors have been fabricated with magnetic permeabilities over 1000.

Summary

The magnetic material developed at SDSM&T has excellent physical properties for the construction of electronic devices that utilize magnetic material. M^3D technology is a method of direct write technology that can effectively manufacture various electronic devices. The physical properties and the low temperature sintering of the devices made in this manner allow for the construction of many novel and experimental devices.

Acknowledgements The silver nano-particle work was performed and supported by the Additive Manufacturing Laboratory (AML) at SDSM&T under grant DAAD19-02-2-001 from the US Army Research Laboratory and the US Army Research Office.

References

1. Marquez GJ, Renn MJ, Miller WD (2002) Mater Res Symp Proc 698:343
2. King B (2003) Electron Packg Prod 43(2):18
3. Renn MJ, Pascal R (1998) J Vac Sci Technol B 16(6):3859
4. Odde DJ, Renn MJ (2000) Biotechnol Bioeng 67:312
5. Odde DJ, Renn MJ (1999) Trends Biotechnol 17:385
6. Miller D et al (2001) HDI 4(9):18
7. Renn MJ et al (2002) In: Pique A, Chrisey DB (eds) Direct-write technologies for rapid prototyping applications: sensors, electronics, and integrated power sources. Academic Press, San Diego, p 475
8. Colvin J, Carter M, Starovoytov O, Puszynski J, Sears J (2005) In: Proceedings of the Materials Science and Technology 2005 Conference, Published in Science and Technology of Powder Materials: Synthesis, Consolidation and Properties, p 63
9. Colvin J, Carter M, Puszynski J, Sears J (2005) In: Proceedings of the International Conference on Applications of Lasers and Electro-Optics (ICALEO-05)
10. Sears J, Colvin J (2005) Proceedings of the 2005 Conference on Powder Metallurgy and Particulate Materials, PM2TEC2005, Montreal, Canada, June 2005
11. Pique A, Chrisey DB (eds) (2002) Direct Write Technologies for Rapid Prototyping Applications. Academic Press, New York
12. Vanheusden K et al (2002) Advancing Microelectron 29(1):1